Proceedings World Geothermal Congress 2020+1
Reykjavik, Iceland, April - October 2021

Numerical Analysis of Heat Extraction Performance of an Open Loop Geothermal System in a Horizontal Well

Gaosheng Wang[1], Xianzhi Song[1]*, Yu Shi[1], Rui Zheng[2], Jiacheng Li[1], Zhen Li[1]

[1]State Key Laboratory of Petroleum Resources and Prospecting, China University of Petroleum, Beijing, Beijing 102249, China

[2]CNPC Engineering Technology R&D Company Limited, Beijing 102206, China

songxz@cup.edu.cn

Keywords: Geothermal Energy, Open Loop, Horizontal Well, Unsteady-state Model, Heat Production Performance

ABSTRACT

An open loop geothermal system (OLGS) in a horizontal well is presented to effectively develop the hydrothermal resources in this paper. Compared with the open loop geothermal system in one vertical well, there is no restriction on the distance between the injection and production intervals for horizontal-well OLGS. Thus, it avoids the early thermal breakthrough and has a broader application prospect, especially for the geothermal exploitation with limited reservoir thickness. However, few studies focus on the performance analysis of horizontal-well OLGS. Hence, a 3D unsteady-state flow and heat transfer model considering the local non-thermal equilibrium (LNTE) is proposed, and it is verified via an analytical solution. Subsequently, the temperature field is investigated, and the effects of key factors on the heat extraction performance of horizontal-well OLGS are studied. The results indicate that the cooling region spreads quickly towards the production section in the early stage. There is an optimal flow rate to obtain higher thermal power with the appropriate temperature of production fluid. The lower inlet temperature is preferred to extract more heat from the reservoir. Furthermore, production pressure plays an important role in heat production. The influence of reservoir porosity is minor. Also, the performance comparison denotes that the horizontal well system can obtain higher production temperature and thermal power than the vertical well system. The main findings of this study can provide guidance for the field application of horizontal-well OLGS.

1. INTRODUCTION

The exploitation of geothermal resource has been attracting wide attention in recent years. As a renewable and clean energy, the geothermal resource is expected to play a more important role in improving air pollution and avoiding energy shortages (Reboredo 2015; Liddle et al. 2017). To reduce the drilling costs and accelerate the development of hydrothermal resource, an open loop geothermal system (OLGS) in a vertical well is proposed, and the injection and production can be completed in one well (Deng et al. 2005; Ni et al. 2011; Ni et al. 2015; Wang et al. 2019). Thus, no additional injection or production well is required. However, the heat output of the vertical well system is relatively limited, especially for the hydrothermal reservoir with restricted thickness. Therefore, an open loop geothermal system (OLGS) in a horizontal well is presented to extract the heat from the reservoir more efficiently.

For the horizontal-well OLGS, the injection section and production section can be perforated in the wellbore near the toe and heel of the horizontal well, respectively, as shown in **Figure 1**. Then, the cooling fluid is injected from the annular space and enters into the reservoir via the injection section. Then the fluid is heated by the high-temperature rock. Afterward, the fluid is produced through the production section and insulation pipe. Compared with the vertical-well system, there is no restriction on the designed length of the injection section, injection-production spacing and production section. Therefore, a serious thermal breakthrough can be avoided. The injection capacity and production capacity can be significantly improved. The horizontal-well OLGS is expected to a better choice to accelerate the exploitation of the hydrothermal resource.

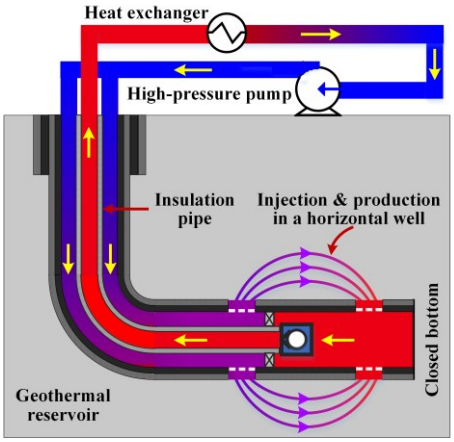

Figure 1: Schematic of heat extraction in horizontal-well OLGS

This paper focuses on the thermal characteristics in the reservoir, while the effect of fluid flow and heat transfer processes in the wellbore is not taken into account. Our study is based on a geothermal field in Tianjin, China, which is full of natural fractures. Hence, the pump pressure can reduce significantly and the fluid can be injected into the formation more easily. Many researchers have carried out a significant amount of investigations on heat extraction in the reservoir. For the reservoir description, the discrete fracture network (DFN) is an effective method to make the factures explicitly embedded into the reservoir (Shaik et al. 2011; Yao et al. 2018; Shi et al. 2019a; 2019b). Sun et al. employed this method to analyze the pressure field and temperature field distributions (Sun et al. 2017). Kolditz adopted the DFN to investigate the thermal characteristics of a 3D model (Kolditz 1995). Furthermore, the equivalent continuous porous medium is also widely adopted to characterize the fractured formation. Jiang et al. analyze the heat transfer process in the reservoir filled with fractures by a single-porosity model (Jiang et al. 2013). Furthermore, to describe the thermal behaviors in the formation, the local thermal equilibrium (LTE) and local non-thermal equilibrium (LNTE) are proposed (Gelet et al. 2013; Heinze et al. 2017; Song et al. 2018). Studies indicated that LTE might not be reliable if the rapid heat exchange between fluid and rock occurs in the fractured formation (Chen et al. 2018). Chen et al. discussed the effect of the rock-fluid heat transfer coefficient according to the LNTE (Chen et al. 2018). Cao et al. established a thermal-hydraulic-mechanical (THM) model considering the LNTE, and found that the lower heat transfer coefficient could lead to the decrease of production temperature (Cao et al. 2016).

To develop the hydrothermal resource more effectively, a horizontal-well OLGS is proposed in this paper. Previous studies have also made significant contributions to comprehend the fluid flow and heat transfer processes in the formation. However, the investigation on the heat extraction performance of horizontal-well OLGS is scarce. Hence, a 3D flow and heat transfer model considering the local non-thermal equilibrium (LNTE) is built, and the model is verified by an analytical solution. Then, the temperature field is discussed. And the production performances under key factors are investigated. Also, the heat outputs of the vertical well system and horizontal well system are compared. The key findings can provide guidance for the field application and optimal design of horizontal-well OLGS.

2. MODEL DESCRIPTION

2.1 Model Assumption

In this paper, the method of the equivalent continuous porous medium is adopted to describe the fractured reservoir, and the reservoir is assumed to be homogeneous and isotropic. The thermophysical properties remain constant and are not affected by the temperature. To obtain more accurate, the theory of local non-thermal equilibrium is applied, which means the temperatures of the fluid and rock at the same point are different. The water serves as the circulation fluid in the horizontal-well OLGS. Based on the reservoir condition (temperature: 85.75~88.75 °C), only single-phase flow behavior is considered in our study. Nevertheless, the temperature influence on the water properties, which can be given by the following equation, while the effect of pressure on the water viscosity is negligible and the pressure is not considered in Eq. (2) (Holzbecher 1998). The influence of pressure on the water density is taken into account in the **Eqs.** (4) and (6).

$$\rho_f = \begin{cases} 1000\times\left(1-\dfrac{\left(T_c-3.98\right)^2}{503570}\times\dfrac{T_c+283}{T_c+67.26}\right) & 0°\text{C}\le T_c\le 20°\text{C} \\ 996.9\times\left(1-3.17\times10^{-4}\times\left(T_c-25\right)-2.56\times10^{-6}\times\left(T_c-25\right)^2\right) & 20°\text{C}\le T_c\le 250°\text{C} \\ 1758.4+10^{-3}T\left(-4.8434\times10^{-3}+T\left(1.0907\times10^{-5}-T\times9.8467\times10^{-9}\right)\right) & 250°\text{C}\le T_c\le 300°\text{C} \end{cases} \tag{1}$$

where *q, k, μ, A, L, and Δp* are volumetric fluid flow rate, absolute permeability, fluid viscosity, cross-sectional area, length and pressure drop over the length *L,* respectively.

$$\mu_f = \begin{cases} 10^{-3}\times\left(1+0.015512\times\left(T_c-20\right)\right)^{-1.572} & 0°\text{C}\le T_c\le 100°\text{C} \\ 0.2414\times10^{\left(\frac{247.8}{T_c+133.15}\right)} & 100°\text{C}\le T_c\le 300°\text{C} \end{cases} \tag{2}$$

where μ_f (Pa·s) is the fluid viscosity.

2.2 Model Assumption

The Darcy's law is employed to characterize the flow behavior in the rock matrix. The mass conservation equation and momentum equation are as follows:

$$\frac{\partial\left(\rho_f\varphi_m\right)}{\partial t}+\nabla\cdot\left(\rho_f u\right)=-Q_f \tag{3}$$

$$\frac{\partial\left(\rho_f\varphi_m\right)}{\partial t}=\varphi_m\frac{\partial\rho_f}{\partial p}\frac{\partial p}{\partial t}+\rho_f\frac{\partial\varphi_m}{\partial p}\frac{\partial p}{\partial t}=\rho_f\varphi_m\left(\chi_f+\chi_s\right)\frac{\partial p}{\partial t} \tag{4}$$

$$u = -\frac{k}{\mu_f}\left(\nabla p - \rho_f g \nabla z\right) \tag{5}$$

where p (Pa) is the pressure. Q_f (kg/(m^3·s)) denotes the mass transfer between the rock matrix and fracture. u (m/s) is the flow velocity in the rock matrix. where φ_m is the porosity of rock matrix. χ_f (1/Pa) is the fluid compressibility, which also represents the effect of pressure on the water density. χ_s (1/Pa) is the rock compressibility. k (m^2) is the permeability of rock matrix. $\rho_f g \nabla z$ is the gravity term, and z represents the vertical direction. Similarly, the fluid flow equation in the fracture is expressed as: Similarly, the fluid flow equation in the fracture is expressed as:

$$\rho_f \varphi_f \left(\chi_f + \chi_s\right) d \frac{\partial p}{\partial t} + \nabla_{\mathrm{T}} \cdot \left(d \rho_f u_f\right) = dQ_f \tag{6}$$

$$u_f = -\frac{k_f}{\mu_f}\left(\nabla_{\mathrm{T}} p - \rho_f g \nabla_{\mathrm{T}} z\right) \tag{7}$$

where d (m) is the fracture aperture. φ_f is the porosity of fracture. ∇_T is the gradient operator restricted to the tangential plane of fracture. u_f (m/s) is the flow velocity in the fracture. k_f (m^2) is the permeability of fracture. Then, the assumption of local thermal non-equilibrium is applied to describe the heat transfer processes in the solid and fluid of the geothermal reservoir. The energy equation in the solid can be determined by:

$$\left(1-\varphi_m\right)\rho_s C_s \frac{\partial T_s}{\partial t} - \nabla \cdot \left(\left(1-\varphi_m\right)\lambda_s \cdot \nabla T_s\right) = -h\left(T_s - T_f\right) \tag{8}$$

where T_s (°C) is the rock temperature. T_f (°C) is the fluid temperature. ρ_s (kg/m^3) is the rock density c_s (J/(kg·ºC)) is the rock thermal capacity. The second term on the left side in **Eq. (8)** corresponds to the heat conduction, and λ_s (W/(m·ºC)) is the rock thermal conductivity. Furthermore, the first term on the right side in **Eq. (8)** represents the heat exchange between the fluid and rock, and h (W/(m^3·ºC)) is the volumetric heat transfer coefficient. Note that h is a variable affected by the flow velocity, fracture aperture, and thermal properties of fluid or rock. Nevertheless, it is commonly assumed to be a constant because the accurate empirical formulas and theoretical solutions are relatively scarce (Jiang et al. 2013; Cao et al. 2016; Chen et al. 2018). Then, the energy equation in the fluid can be given by:

$$\varphi_m \rho_f C_f \frac{\partial T_f}{\partial t} + \rho_f C_f u \cdot \nabla T_f - \nabla \cdot \left(\varphi_m \lambda_f \cdot \nabla T_f\right) = h\left(T_s - T_f\right) \tag{9}$$

where c_f (J/(kg·ºC)) is the fluid thermal capacity. The second term on the left side in **Eq. (9)** represents the heat convection. λ_f (W/(m·ºC)) is the fluid thermal conductivity. Similarly, the heat transfer equation in the fracture is written as:

$$\varphi_f d \rho_f C_f \frac{\partial T_f}{\partial t} + d \rho_f C_f u_f \cdot \nabla_{\mathrm{T}} T_f = dh\left(T_s - T_f\right) \tag{20}$$

Note that the thermal convection is dominant in the fracture due to the high-velocity flow of injection fluid. Hence, the effect of thermal conduction is neglected in this region. Moreover, the heat extraction rate can be calculated by:

$$P = 10^{-6} \cdot \left(M_{out} C_{f,out} T_{out} - M_{in} C_{f,in} T_{in}\right) \tag{31}$$

where P (MW) is the thermal power. M (m^3/s) is the mass flow rate. The subscripts *in* and *out* are the variables at the inlet and outlet, respectively.

2.3 Model Verification

To verify the reliability of the numerical model proposed in our paper, the analytical solution describing fluid flow and heat transfer processes in a 2D single fracture is employed (Barends 2010). **Figure 2** illustrates that the numerical solutions at 30 d, 60 d, and 120 d agree well with the analytical solutions. This indicates that our model is quite reliable, and it can be utilized to analyze the thermal characterizes of the horizontal-well OLGS.

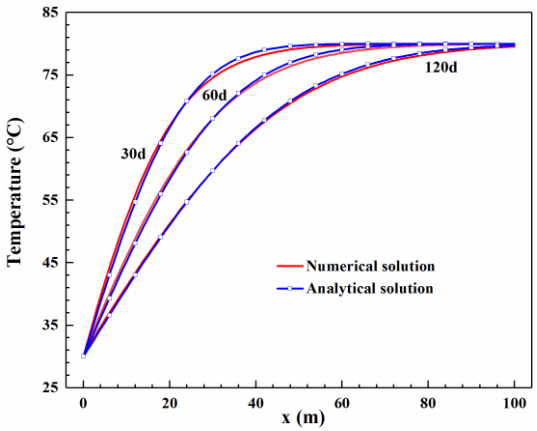

Figure 2: Comparison between the numerical solution and analytical solution in a 2D single fracture

2.4 Computational Model

This study focuses on the geothermal field in Dongli region, Tianjin, China. Based on geological data, the geometric model is shown in **Figure 3**, which is consists of the overlying layer, reservoir, and underlying layer. The computational dimensions of the geometric model are 400 m × 400 m × 150 m, and the thicknesses of the overlying layer and underlying layer are 25 m. Besides, the injection-production spacing is set as 50 m, which represents the distance between the injection section (blue line segment) and the production section (red line segment). Note that 50 m also serves as the lengths of injection and production sections. Furthermore, the hydraulic fractures are uniformly distributed along the injection and production sections. The geometric parameters are listed in **Table 1**.

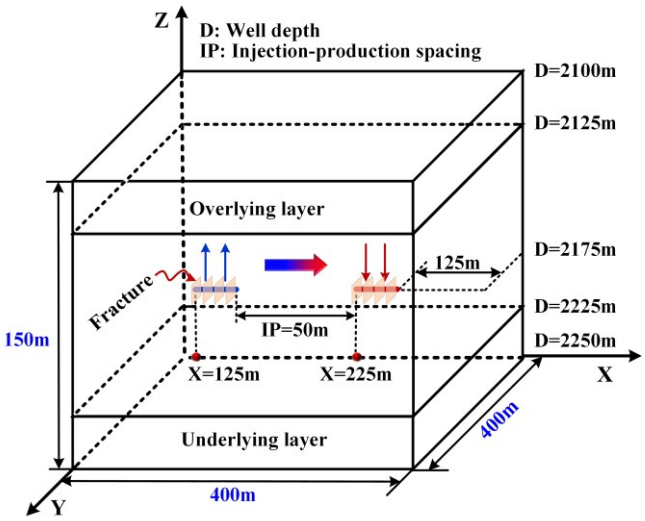

Figure 3: Schematic of geometric model in horizontal-well OLGS

It should be noted that the reservoir lithology is limestone, and a large number of natural fractures exist in the formation. To reduce the computational load, a common method is to assume the formation as the equivalent continuous porous medium. This assumption is also adopted in this study, and the physical parameters of the formation are displayed in **Table 2** (Kell 1975; Ahmed 2006). Note that the fracture is considered to be full of water, thus the thermophysical properties are the same as the water. And Based on the references (Jiang et al. 2013; Cao et al. 2016; Chen et al. 2018), the rock-fluid volumetric heat transfer coefficient is set as 1 (W/(m^3·°C)).

Table 1 Geometrical parameters of the numerical model

Items	Values
Computational dimensions	400 m × 400 m × 150 m
Reservoir dimensions	400 m × 400 m × 100 m
Wellbore diameter (m)	0.2699
Fracture aperture (m)	0.001
Fracture width (m)	40
Fracture length (m)	40
Fracture spacing (m)	7
Injection interval (m)	50
Production interval (m)	50
Injection-production spacing (m)	50

Table 2 Formation physical properties

Items	Overlying layer	Reservoir rock	Underlying layer	Fracture
Density (kg/m^3)	2600	2500	2600	-
Thermal capacity (J/(kg·°C))	850	870	850	-
Thermal conductivity (W/(m·°C))	2.1	3	2.1	-
Porosity (%)	3	7	3	100
Permeability (m^2)	10^{-16}	10^{-13}	10^{-16}	10^{-11}
Compressibility [10^{-10}/Pa]	12.0076	8.2848	12.0076	4.6748

2.5 Initial and Boundary Conditions

As shown in **Figure 3**, the depth of the geometric model ranges from 2100 m to 2250 m. Thus, the pressure at the top boundary is set as 20.29 MPa according to the geological conditions, and the pressure in the formation increases linearly along the vertical direction with a pressure gradient of 9480 Pa /m. Moreover, the temperature at the top of the geometric model is 85 °C, and the geothermal gradient is 0.03 °C/m. Note that the adiabatic condition and no-flow condition are applied on the side boundaries. In terms of the field conditions, the injection flow rate and injection temperature of the working fluid are 45 kg/s and 35 °C, respectively. And the computational time is set as 120 d based on the building heating regulations in the north of China. Then, the finite element solver COMSOL is applied to solve the mathematical model. And the segregated coupled approach is employed to achieve better convergence of the nonlinear equations. This makes it possible to split the solution process into substeps, and each substep uses a damped version of Newton's method.

3. ANALYSIS OF THE TEMPERATURE FIELD

Figure 4 illustrates the temperature distribution in the geothermal reservoir under various production times. It is clear that the low-temperature region expands quickly from the injection section to the production section in the early stage. And the thermal breakthrough can be observed after 30 days, which can lead to a rapid decrease of the production temperature. Then, the region with low temperature tends to spread toward the radial direction near the injection section. Consequently, the geometry of the low-temperature region is similar to a circle. Besides, the impact scope of the low-temperature region is relatively limited, which also indicates that the boundaries conditions have little effect on the numerical results.

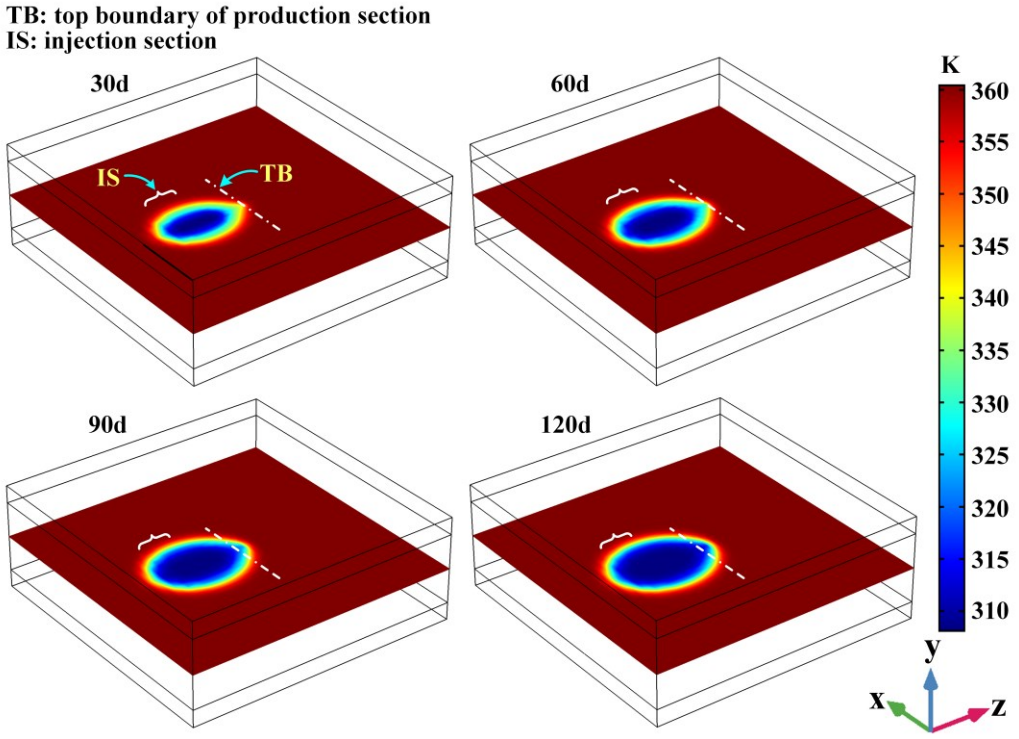

Figure 4: Temperature distribution in the reservoir under different production times

4. PERFORMANCE COMPARISON OF VERTICAL WELL AND HORIZONTAL WELL SYSTEMS

In this section, the heat extraction performance of vertical well and horizontal well systems are compared. **Figure 5** displays the schematic of the geometric model in vertical-well OLGS, which is different from that in horizontal-well OLGS. And its injection section and production section are perforated in the upper and lower wellbore. The fractures distribution is the same as that in the horizontal well system, but it is not shown in **Figure 5**. The total vertical length of the injection section, injection-production spacing, and production section is 100 m. Apparently, the lengths of the injection section and production section play an important role in the injection capacity and production capacity, respectively. And the injection-production spacing is closely related to the thermal breakthrough. Hence, the lengths of the injection section and production section are both set as 30 m, which aims at showing a relatively good performance. Note that the lengths of the injection section, injection-production spacing, and production section are not the same as that of the horizontal-well OLGS. This is because the thickness of the reservoir is relatively limited. It

also means that the horizontal-well OLGS has a broader prospect in developing the hydrothermal resources with relatively limited thickness.

Figure 6 depicts the performance comparison of vertical-well OLGS and horizontal-well OLGS. It can be observed that the production temperature of the vertical well system is higher than that of the horizontal well system within 3 days. The reason is that the production section of the vertical well system is lower, and more high-temperature fluid can be extracted in the early period. Then, due to the serious thermal breakthrough, the production temperature of vertical-well OLGS reduces more sharply, and the maximum temperature difference compared to the horizontal well system is about 9.55 ° C. Also, the thermal power of the vertical well system is much lower than that of the horizontal-well OLGS, and the thermal power difference after 120 days is around 2.01 MW. Thus, it can be concluded that the horizontal-well OLGS may be a better choice to accelerate the exploitation of hydrothermal resources.

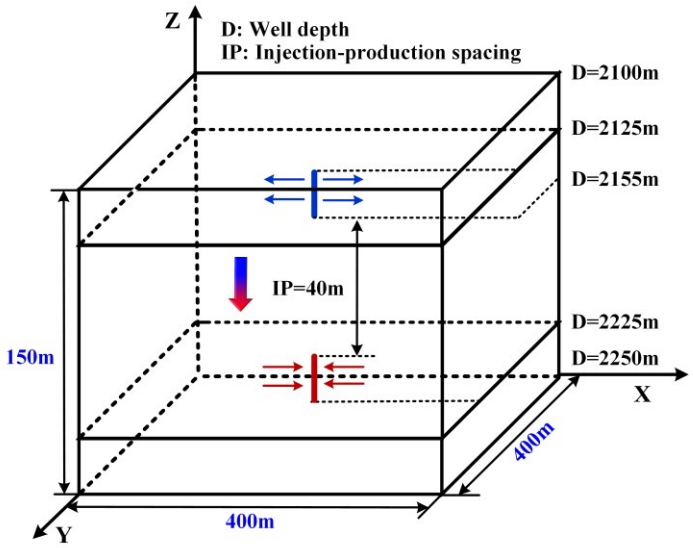

Figure 5: Schematic of geometric model in vertical-well OLGS

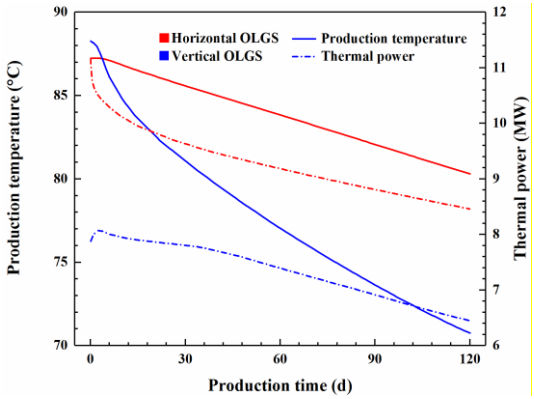

Figure 6: Performance comparison of vertical-well OLGS and horizontal-well OLGS

5. INFLUENCES OF KEY FACTORS ON HEAT EXTRACTION PERFORMANCE

In this section, the influence of key factors, including the injection flow rate, injection fluid temperature, production pressure, and reservoir porosity, on the heat extraction performance of horizontal-well OLGS are analyzed to provide a significant reference for its optimum design.

5.1 Influences of Injection Flow Rate

Figure 7. Illustrates the production temperature and thermal power with production time under various injection flow rates. It is clear that a higher injection flow rate can lead to a more serious thermal breakthrough, and the production temperature differences with different injection flow rates increase as the production continues. And the maximum production outlet temperature is approximately 7.60 ° C when the injection mass flow ranges from 25kg/s to 65 kg/s. However, higher thermal power can be obtained if more fluid is injected into the reservoir. And the thermal power difference after 120 days is around 5.98 MW. In this paper, the default injection flow rate is set as 45 kg/s. And it can be observed the heat output is relatively stable. Meanwhile, the production temperature and thermal power with 45 kg/s are about 80.30 ° C and 8.46 MW separately, which satisfy the requirements of spacing heating. Hence, the injection flow rate of 45 kg/s is also adopted in the following study.

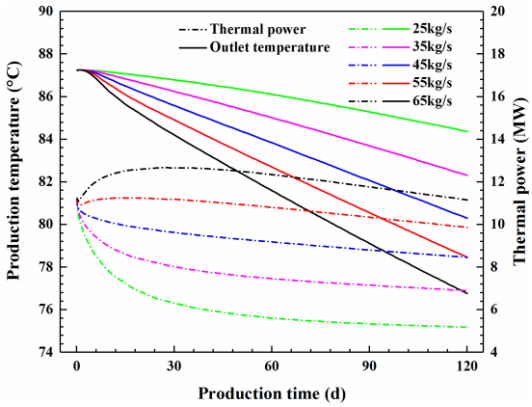

Figure 7: Production temperature and thermal power under various injection flow rates

5.2 Influences of Injection Fluid Temperature

Figure 8 shows the production temperature and thermal power with production time under various injection fluid temperatures. Obviously, the production temperature decreases gradually if a lower injection fluid temperature is applied. However, this can lead to an enormous increase of thermal power. Compared to the heat output with the injection fluid temperature of 45 ° C, the maximum increase range reaches 50.36 %. Hence, we should reduce the temperature of injection fluid as far as possible in the field if the production temperature meets the requirements of the building heating.

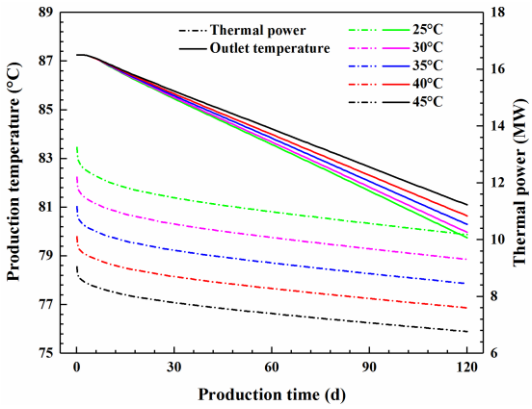

Figure 8: Production temperature and thermal power under various injection fluid temperatures

5.3 Influences of Production Pressure

Figure 9 displays the production temperature and thermal power with production time under various production pressures. It can be observed that the influence of production pressure on the production temperature is minor. However, the thermal powers with different production pressures have an obvious change in the early stage. And the maximum thermal power difference can reach around 16.04 MW when the production pressure decreases from 20.29 MPa to 16.29 MPa. It is recommended to employ a lower production pressure in the application of horizontal-well OLGS.

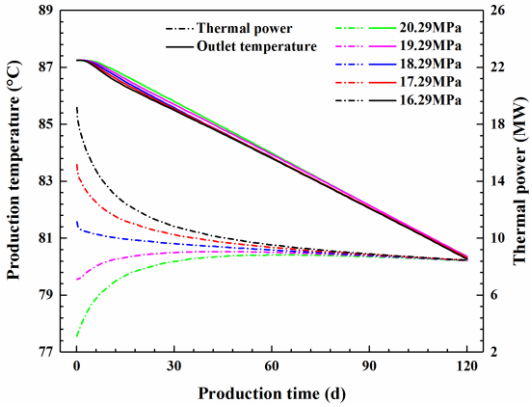

Figure 9: Production temperature and thermal power under various production pressures

5.4 Influences of Reservoir Porosity

Figure 10 depicts the production temperature and thermal power with production time under various reservoir porosities. Obviously, the thermal breakthrough appears earlier with the decrease of the reservoir porosity. The main reason for the variation of production temperature is that the reservoir is filled with more high-temperature geothermal fluid when the porosity rises, which makes the reservoir temperature more difficult to change. Therefore, the thermal power with the porosity of 0.25 can reach approximately 8.84 MW, which is 0.48 MW higher than that with the porosity of 0.03. Compared to the influences of other factors, the reservoir porosity does not play a noticeable role in the heat extraction process of the horizontal well system.

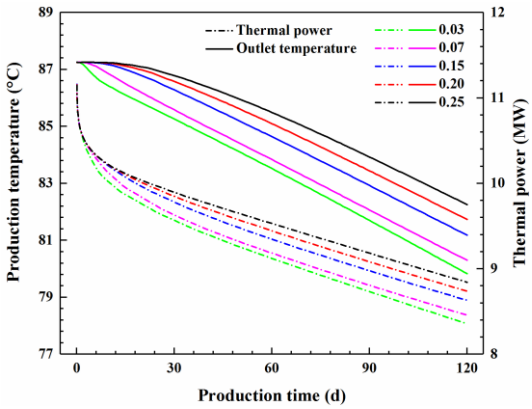

Figure 10: Production temperature and thermal power under various reservoir porosities

6. CONCLUSIONS

In this paper, an open loop geothermal system (OLGS) in a horizontal well is proposed to develop the hydrothermal resources more effectively. Compared with the open loop geothermal system in one vertical well, the length of the injection section, production section, and injection-production section have no restriction. Thus, the injection capacity production capacity can be improved, and the thermal breakthrough can be delayed. Subsequently, a 3D unsteady-state flow and heat transfer model considering the local non-thermal equilibrium (LNTE) is established. The temperature field and the influences of vital factors on heat extraction performance are investigated. Furthermore, the heat productions of vertical-well OLGS and horizontal-well OLGS are compared. The main findings are as follows:

- The temperature field investigation shows that the cooling region spreads quickly towards the production section. And a thermal breakthrough can be seen after a certain production time. Moreover, the impact scope of the low-temperature region is relatively limited, which denotes that more horizontal-well OLGSs may be required to exploit the geothermal resources of the reservoir thoroughly.

- The higher injection flow rate can lead to a serious thermal breakthrough, but it is beneficial to improve the heat output. Meanwhile, there is a flow rate to obtain relatively stable production curves. The injection fluid temperature has a significant influence on the heat output. And a lower injection fluid temperature is preferred.

- The effect of reservoir porosity on heat extraction performance is minor. The production pressure can greatly improve the heat production capacity in the early stage, while the temperature of production fluid has little change. And the lower production pressure is recommended in the field application of the horizontal-well system.

- The performance comparison indicates that the thermal breakthrough occurs earlier in the vertical-well OLGS, while the production temperature and thermal power of horizontal-well OLGS are higher than that of the vertical well system in the vast majority of production time. Particularly, the increase ranges of production temperature and thermal power under our simulation conditions can reach around 13.50% and 31.16%, respectively. Hence, the horizontal well system is expected to be a better choice to exploit hydrothermal resources.

ACKNOWLEDGEMENTS

The authors would like to acknowledge the National Key R&D Program of China (Grant No. 2018YFB1501804), National Natural Science Funds for Excellent Young Scholars of China (Grant No. 51822406), Program of Introducing Talents of Discipline to Chinese Universities (111 Plan) (Grant NO. B17045), and the Beijing Outstanding Young Scientist Program (Grant NO. BJJWZYJH012019114140 38).

REFERENCES

Ahmed, T.: Reservoir engineering handbook, *Elsevier*, (2006).

Barends, F.: Complete solution for transient heat transport in porous media, following Lauwerier. *SPE Annual Technical Conference and Exhibition*. Society of Petroleum Engineers, (2010).

Cao, W., Huang, W., and Jiang, F.: A novel thermal–hydraulic–mechanical model for the enhanced geothermal system heat extraction, *International Journal of Heat and Mass Transfer*, 100, (2016), 661-671.

Chen, Y., Ma, G., Wang, H., and Li, T.: Evaluation of geothermal development in fractured hot dry rock based on three dimensional unified pipe-network method, *Applied Thermal Engineering*, 136, (2018), 219-228.

Deng, Z., Rees, S. J., and Spitler, J. D: A model for annual simulation of standing column well ground heat exchangers, *Hvac&R Research*, 11(4), (2005), 637-655.

Gelet, R., Loret, B., and Khalili, N.: Thermal recovery from a fractured medium in local thermal non‐equilibrium, *International Journal for Numerical and Analytical Methods in Geomechanics*, 37(15), (2013), 2471-2501.

Heinze, T., and Hamidi, S.: Heat transfer and parameterization in local thermal non-equilibrium for dual porosity continua, *Applied Thermal Engineering*, 114, (2017), 645-652.

Holzbecher, E. O.: Modeling density-driven flow in porous media: principles, numerics, software] *Springer Science & Business Media*, (1998).

Jiang, F., Luo, L., and Chen, J.: A novel three-dimensional transient model for subsurface heat exchange in enhanced geothermal systems, *International communications in heat and mass transfer*, 41, (2013), 57-62.

Kell, G.S.: Density, thermal expansivity, and compressibility of liquid water from 0. deg. to 150. deg. Correlations and tables for atmospheric pressure and saturation reviewed and expressed on 1968 temperature scale, *Journal of Chemical and Engineering Data*, 20, (1975), 97-105.

Kolditz, O.: Modelling flow and heat transfer in fractured rocks: conceptual model of a 3-D deterministic fracture network, *Geothermics*, 24(3), (1995), 451-470.

Liddle, B., and Sadorsky, P.: How much does increasing non-fossil fuels in electricity generation reduce carbon dioxide emissions?, *Applied energy*, 197, (2017), 212-221.

Ni, L., Li, H., Jiang, Y., Yao, Y., and Ma, Z.: A model of groundwater seepage and heat transfer for single-well ground source heat pump systems, *Applied Thermal Engineering*, 31(14-15), (2011), 2622-2630.

Ni, L., Dong, J., Yao, Y., Shen, C., Qv, D., and Zhang, X.: A review of heat pump systems for heating and cooling of buildings in China in the last decade, *Renewable Energy*, 84, (2015), 30-45.

Reboredo, J.C.: Renewable energy contribution to the energy supply: Is there convergence across countries?, *Renewable and Sustainable Energy Reviews*, 45, (2015), 290-295.

Shaik, A. R., Rahman, S. S., Tran, N. H., and Tran, T.: Numerical simulation of fluid-rock coupling heat transfer in naturally fractured geothermal system, *Applied thermal engineering*, 31(10), (2011), 1600-1606.

Shi, Y., Song, X., Wang, G., McLennan, J., Forbes, B., Li, X., and Li, J.: Study on wellbore fluid flow and heat transfer of a multilateral-well CO2 enhanced geothermal system, *Applied Energy*, 249, (2019a), 14-27.

Shi, Y., Song, X., Wang, G., Li, J., Geng, L., and Li, X.: Numerical study on heat extraction performance of a multilateral-well enhanced geothermal system considering complex hydraulic and natural fractures, *Renewable Energy*, 141, (2019b), 950-963.

Song, X., Shi, Y., Li, G., Yang, R., Wang, G., Zheng, R., Li, J., and Lyu, Z.: Numerical simulation of heat extraction performance in enhanced geothermal system with multilateral wells, *Applied energy*, 218, (2018), 325-337.

Sun, Z., Zhang, X., Xu, Y., Yao, J., Wang, H., Lv, S., Sun, Z., Huang, Y., Cai, M., and Huang, X.: Numerical simulation of the heat extraction in EGS with thermal-hydraulic-mechanical coupling method based on discrete fractures model, *Energy*, 120, (2017), 20-33.

Wang, G., Song, X., Shi, Y., Sun, B., Zheng, R., Li, J., Pei, Z., and Song, H.: Numerical investigation on heat extraction performance of an open loop geothermal system in a single well, *Geothermics*, 80, (2019), 170-184.

Yao, J., Zhang, X., Sun, Z., Huang, Z., Liu, J., Li, Y., Xin, Y., Yan, X., and Liu, W.: Numerical simulation of the heat extraction in 3D-EGS with thermal-hydraulic-mechanical coupling method based on discrete fractures model, *Geothermics*, 74, (2018), 19-34.